

Cite this: *Dalton Trans.*, 2018, **47**, 4707

## Combining covalent bonding and electrostatic attraction to achieve highly viable species with ultrashort beryllium–beryllium distances: a computational design†

Zhen-Zhen Qin,<sup>a</sup> Qiang Wang,<sup>b</sup> Caixia Yuan,<sup>a</sup> Yun-Tao Yang,<sup>a</sup> Xue-Feng Zhao,<sup>a</sup> Debao Li,<sup>b</sup> Ping Liu<sup>b</sup> and Yan-Bo Wu<sup>\*a,b</sup>

Though ultrashort metal–metal distances (USMMD,  $d_{M-M} < 1.900 \text{ \AA}$ ) were primarily realized between transition metals, USMMDs between main group metal atoms such as beryllium atoms have also been designed previously using two strategies: (1) formation of multiple bonding orbitals or (2) having favourable electrostatic attraction. We recently turned our attention to the reported species  $\text{IH} \rightarrow \text{Be}_2\text{H}_2 \leftarrow \text{IH}$  (where IH denotes imidazol-2-ylidene) because the orbital energy level of its  $\pi$ -type HOMO is noted to be very high, which may result in intrinsic instability. In the present study, we combined the abovementioned strategies to solve the high orbital energy level problem without losing the ultrashort Be–Be distances. It was found that breaking of such  $\pi$ -type HOMO by addition of a  $-\text{CH}_2-$  group onto the bridging position of two beryllium atoms led to the formation of  $\text{IH} \rightarrow \text{Be}_2\text{H}_2\text{CH}_2 \leftarrow \text{IH}$  species, which not only possesses an ultrashort Be–Be distance in the  $-\text{Be}_2\text{H}_2\text{CH}_2-$  moiety, but also has a relatively low HOMO energy level. Replacing the IH ligands with  $\text{NH}_3$  and  $\text{PH}_3$  resulted in the formation of  $\text{NH}_3 \rightarrow \text{Be}_2\text{H}_2\text{CH}_2 \leftarrow \text{NH}_3$  and  $\text{PH}_3 \rightarrow \text{Be}_2\text{H}_2\text{CH}_2 \leftarrow \text{PH}_3$  species with similar features. The electronic structure analyses suggest that the ultrashort Be–Be distances in these species are achieved by the combined effects of the formation of two Be–H–Be 3c-2e bonds and having favourable Coulombic attractions between the carbon atom of the  $-\text{CH}_2-$  group and two beryllium atoms. Remarkably, when the IH,  $\text{NH}_3$ , and  $\text{PH}_3$  ligands were replaced by large ligands with bulky groups, such as 1,3-bis(2,6-diisopropyl phenyl)imidazol-2-ylidene (IDip), triphenylamine ( $\text{NPh}_3$ ), and triphenylphosphine ( $\text{PPh}_3$ ), respectively, the resultant species  $\text{IDip} \rightarrow \text{Be}_2\text{H}_2\text{CH}_2 \leftarrow \text{IDip}$ ,  $\text{NPh}_3 \rightarrow \text{Be}_2\text{H}_2\text{CH}_2 \leftarrow \text{NPh}_3$ , and  $\text{PPh}_3 \rightarrow \text{Be}_2\text{H}_2\text{CH}_2 \leftarrow \text{PPh}_3$  exhibit good steric protection around the  $-\text{Be}_2\text{H}_2\text{CH}_2-$  core. These species are thus examples for the experimental realization of species with ultrashort metal–metal distances between main group metals.

Received 27th December 2017,

Accepted 26th February 2018

DOI: 10.1039/c7dt04897a

rsc.li/dalton

## Introduction

Scientists are generally interested in the utmost limits of various topics. In metal–metal bonding chemistry, an often asked question is “how short a metal–metal bond can become?” Such a query has intrigued chemists for more than five decades since Cotton *et al.*<sup>1</sup> proposed, in 1964, the first

metal–metal quadruple bond with a rather short rhenium–rhenium distance of  $2.24 \text{ \AA}$  in  $\text{Re}_2\text{Cl}_8^{2-}$ . In 2005, Power *et al.* reported a crystalline structure with a chromium–chromium quintuple bond and a surprisingly short chromium–chromium distance of  $1.835 \text{ \AA}$ .<sup>2,3</sup> Such interesting findings caused sensation at that time and sparked considerable efforts to achieve even shorter metal–metal distances.<sup>4,5</sup> For crystalline structures, metal–metal distances as short as  $1.706 \text{ \AA}$ <sup>6–13</sup> have been realized between two chromium atoms. In addition, computationally designed species with metal–metal distances as short as  $1.650 \text{ \AA}$  were also achieved between two chromium atoms.<sup>14–17</sup> Chromium can be a good choice because it is the smallest among the group 6 elements, which can form a homo-nuclear quintuple bond.

However, achieving the ultrashort metal–metal distances between main group metals is not as straightforward. Though a maximum bond order of three can be obtained for main

<sup>a</sup>Key Lab of Materials for Energy Conversion and Storage of Shanxi Province, Institute of Molecular Science, Shanxi University, Taiyuan, Shanxi, 030006, China. E-mail: wyb@sxu.edu.cn

<sup>b</sup>State Key Lab of Coal Conversion, Institute of Coal Chemistry, Chinese Academy of Sciences, Taiyuan, Shanxi, 030001, China

†Electronic supplementary information (ESI) available: The comparative AdNDP and CMO results of **B1** versus **B1'** and **C1** versus **C1'**, the tables summarizing the lowest vibrational frequencies, the orbital energy levels, the NBO results, and the Cartesian coordinates of all the species reported in this work. See DOI: 10.1039/c7dt04897a

group elements, a classical homo-nuclear triple bond (involving a two-center two-electron ( $2c-2e$ )  $\sigma$  bond and two  $2c-2e$   $\pi$  bonds) has not been observed between main group metals because s-block metals do not have enough valence electrons and the outermost s-electron-pairs in p-block metals are rather inert due to relativistic effects. Nevertheless, beryllium (Be), the smallest metal in the Periodic table, is an exception among the main group metals as it shows distinct electron deficient properties. Therefore, it is possible to form multiple bonding orbitals between two beryllium atoms with the aid of appropriate bridging atoms, which can significantly shorten the Be–Be distances.

Such a potential had been explored recently. Ding *et al.* and Frenking *et al.* designed the  $\text{Be}_2\text{B}_8$  ( $D_{8h}$ ) and  $\text{Be}_2\text{B}_7^-$  ( $D_{7h}$ ) molecular discs with unusually short Be–Be distances of 1.910 and 1.901 Å,<sup>18</sup> respectively. Such Be–Be distances are the result of the combined effect of three relatively stronger  $\sigma$ -bonding orbitals and three relatively weaker  $\pi$ -anti-bonding orbitals. Our group designed the 3D molecular stars  $\text{Be}_2\text{CBe}_5\text{H}_5^+$  and  $\text{Be}_2\text{CBe}_6\text{H}_6^{2+}$  with very short axial Be–Be distances of 1.776 and 1.802 Å,<sup>19</sup> respectively, which result from the combined effect of three relatively stronger  $\sigma$ -bonding orbitals and one relatively weaker  $\pi$ -anti-bonding orbital. In addition, we also designed a series of species with rhombic  $\text{Be}_2\text{X}_2$  cores and short Be–Be distances between 1.866 and 1.728 Å but without a bonding orbital between the two beryllium atoms.<sup>19,20</sup> The ultrashort Be–Be distances are achieved by the strong Coulombic attractions between the X and Be atoms. The majority of these species possess global energy minima and are thus promising targets for gas-phase generation and characterization.

The more interesting species is  $\text{IH} \rightarrow \text{BeH}_2\text{Be} \leftarrow \text{IH}$  (*e.g.*, **A1** in Fig. 1), where IH denotes the small model N-heterocyclic carbene (NHC) ligand imidazol-2-ylidene. In this species, the

IH ligands donate a pair of electrons to each beryllium atom, so that the valence electrons of beryllium can be used to form orbitals for Be–Be bonding. Furthermore, with the aid of bridging hydrogen atoms, three bonding orbitals are formed, so that the Be–Be distances are shortened to about 1.830 Å.<sup>19</sup> If the IH ligand has a bulky group, the corresponding structure (*e.g.*, **A2** in Fig. 1) provides steric protection to the  $-\text{BeH}_2\text{Be}-$  core, leading to a seemingly potential synthetic target with ultrashort main group metal–metal distances.

However, our electronic structure analyses on **A1** suggest that the energy level of its HOMO is very high, which would lead to high reactivity and a small HOMO–LUMO gap, *i.e.*, such a molecule may be not stable enough for experimental realization. Since the HOMO is one of three bonding orbitals that contribute to shortening of the Be–Be distance, if directly eliminated, the ultrashort Be–Be distance will disappear simultaneously. Therefore, to solve the problem raised by the high energy level HOMO without losing the ultrashort Be–Be distance, an appropriate scheme is required. In this study, we attempted to combine the strategies of forming multiple bonding orbitals and having favourable electrostatic attractions for obtaining ultrashort Be–Be distance. As we show below, breaking the  $\pi$ -type HOMO by adding a  $-\text{CH}_2-$  group at the bridging position between two beryllium atoms leads to the formation of a species that not only possesses ultrashort Be–Be distance in the  $-\text{Be}_2\text{H}_2\text{CH}_2-$  moiety, but also possesses HOMO with relatively low energy levels.

## Computational methods

The species investigated in this study were optimized and characterized as minimum-energy structures at the B3LYP/BS1 level, where BS1 denotes the aug-cc-pVTZ (cc-pVTZ for **A1'**)

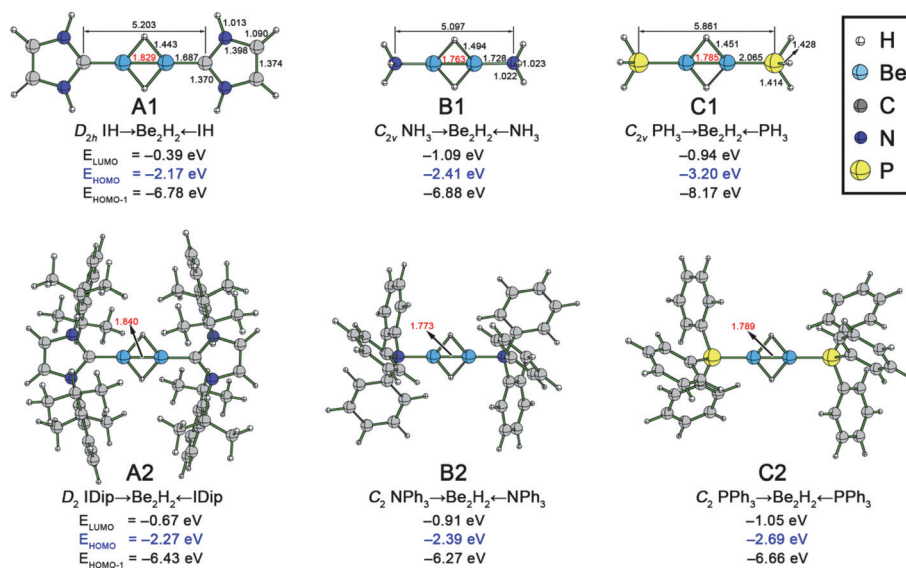


Fig. 1 CCSD(T)/BS1-optimized structures of **A1**–**C1** and B3LYP/BS1-optimized structures of **A2**–**C2**. The bond lengths or interatomic distances are given in angstrom.

basis set for beryllium and the atoms bonded to beryllium, while the cc-pVDZ basis set was used for all other atoms. For the small model structures, the B3LYP/BS1 results were calibrated using the double hybrid functional B2PLYP-D3<sup>21,22</sup> in combination with the BS1 basis set, which provided similar results. The structures of the small models were further refined at the CCSD(T)/BS1 level, generating similar geometries. The CCSD(T)/BS1 geometries of the small models and the B3LYP/BS1 geometries of the large molecules are reported in the text. To better understand the electronic structure, the orbital energy level, canonical molecular orbital (CMO), and natural bond orbital (NBO)<sup>23</sup> analyses were performed at the B3LYP/BS1 level, while the adaptive natural density partitioning (AdNDP)<sup>24,25</sup> analyses were carried out at the B3LYP/6-31G level. The AdNDP analyses were performed using the AdNDP program,<sup>26</sup> the CCSD(T) calculations were performed using the MolPro 2012.1 package,<sup>27</sup> and all other calculations were carried out using the Gaussian 09 package.<sup>28</sup>

## Results and discussion

### Orbital analyses

Previously, we had performed the AdNDP analyses on **A1**. As shown in Fig. 2, **A1** possesses two C → Be dative bonds with occupation numbers (ONs) of 1.96|e|. The existence of these two bonds makes it possible for the two beryllium atoms to use all their valence electrons for Be–Be interactions. Consistently, with the aid of bridging hydrogen atoms, two Be–H–Be three-center two-electron (3c-2e) bonds (ONs = 1.96|e|) and a C–Be–Be–C four-center two-electron (4c-2e) π-bond

(ON = 2.00|e|) are formed. These three bonding orbitals contribute to shortening the Be–Be distance to 1.829 Å. In this study, we established the relationship between the AdNDP-partitioned orbitals and the canonical molecular orbitals (CMOs). As shown in Fig. 2, two Be–H–Be 3c-2e bonds combine to obtain the COMs HOMO–3/HOMO–8, while two C → Be 2c-2e dative bonds combine to obtain the CMOs HOMO–6/HOMO–7. These four CMOs possess rather low orbital energy levels. In contrast, the AdNDP-partitioned C–Be–Be–C 4c-2e π-bond is not significantly combined with other orbitals as demonstrated by its almost identical orbital shape to that of the HOMO in **A1**. Since the carbon-to-carbon distance along the C–Be–Be–C axis is 5.203 Å (Fig. 1), it is necessary for the orbitals delocalized over such a long distance to have very high energy levels, so that the electrons are less bounded to the nuclei. Consistently, the HOMO energy level of **A1** is –2.17 eV at the B3LYP/BS1 level, which is only 1.78 eV lower than that of the LUMO. As the HOMO–1 of **A1** is 4.51 eV lower in energy than the HOMO, if the HOMO energy level of **A1** can be lowered or if the electrons in the HOMO can be directed into the lower energy orbitals, it would be possible to solve the problem caused by high energy HOMO.

### Using different electron donors

First, to stabilize the –Be<sub>2</sub>H<sub>2</sub>– core, we tried to alter the HOMO energy levels by using two electron-donating ligands NH<sub>3</sub> and PH<sub>3</sub>. As shown in Fig. 1, substituting the IH ligand in **A1** with NH<sub>3</sub> or PH<sub>3</sub> ligand led to the formation of new structures NH<sub>3</sub> → BeH<sub>2</sub>Be ← NH<sub>3</sub> (**B1**) or PH<sub>3</sub> → BeH<sub>2</sub>Be ← PH<sub>3</sub> (**C1**), respectively. At both the B3LYP/BS1 and B2PLYP-D3/BS1 levels, **B1** and **C1** are confirmed to be minimum-energy structures.

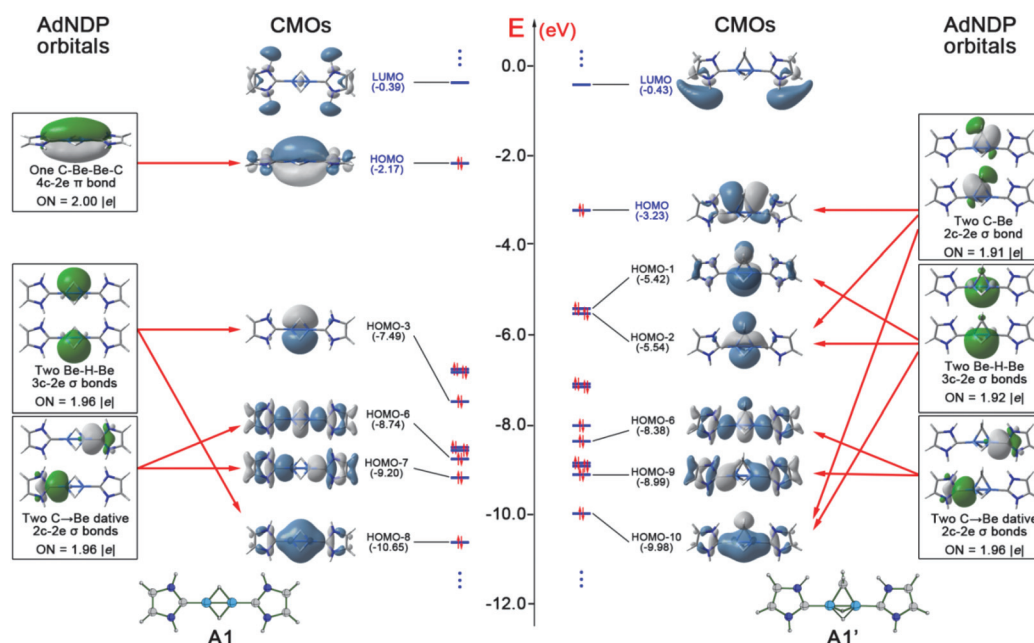


Fig. 2 The comparative AdNDP and CMO analyses of **A1** versus **A1'**. Two phases of AdNDP and CMO orbitals are shown in green/white and blue/white, respectively.

The CCSD(T)/BS1-optimized Be–Be distances of 1.763 and 1.785 Å in **B1** and **C1**, respectively, are even shorter than that in **A1** (1.829 Å). Nevertheless, relative to the energy levels of LUMOs of **B1** and **C1** (−1.09 and −0.94 eV), the energy levels of their HOMOs (−2.41 and −3.20 eV) are still very high. In addition, the orbital analyses also revealed that **B1** and **C1** both possess a high energy  $\pi$ -HOMO, which is similar in shape to that of **A1** (see Fig. S1 and S2 in ESI†). These results suggest that changing the type of electron donating ligands cannot substantially lower the energy level of  $\pi$ -shape HOMOs.

Next, we examined bulky electron donating ligands expecting that the bigger ligands would lower the HOMO energy levels. Bulky groups can significantly improve the stability of species, as exemplified by the all-*meta-tert*-butyl derivatives of hexaphenylethane.<sup>29</sup> In this study, we replaced the IH, NH<sub>3</sub>, and PH<sub>3</sub> ligands in **A1–C1** with the commonly employed 1,3-bis(2,6-diisopropyl phenyl)imidazol-2-ylidene (IDip), triphenylamine (NPh<sub>3</sub>), and triphenylphosphine (PPh<sub>3</sub>) ligands, respectively, resulting in the IDip → Be<sub>2</sub>H<sub>2</sub> ← IDip (**A2**) NPh<sub>3</sub> → Be<sub>2</sub>H<sub>2</sub> ← NPh<sub>3</sub> (**B2**), and PPh<sub>3</sub> → Be<sub>2</sub>H<sub>2</sub> ← PPh<sub>3</sub> (**C2**) species (Fig. 1). At the B3LYP/BS1 level, they are computed to be minimum-energy structures with ultrashort Be–Be distances of 1.840, 1.773, and 1.789 Å, respectively. As shown in Fig. 1, though the –Be<sub>2</sub>H<sub>2</sub>– moieties in these species are partially protected by the bulky groups, the HOMO energy levels of **A2–C2** (−2.27, −2.39, and −2.69 eV, respectively) are similar to or even higher than those of **A1–C1**. Correspondingly, the HOMO–LUMO gaps of **A2–C2** are also small, being 1.60, 1.48, and 1.64 eV, respectively. Such results indicate that electron donors with bulky protecting groups hardly affect the HOMO energy levels.

### Directing the electrons in the HOMO into low-lying orbitals

Since the HOMOs of **A1–C1** are all  $\pi$ -orbitals delocalized over the X–Be–Be–X (X = C, N, P) moieties, it is reasonable to con-

sider that **A1–C1** have “unsaturated” cores. In organic chemistry, unsaturated hydrocarbons can be stabilized on saturation. Therefore, we applied the concept of “saturation” from organic chemistry to stabilize the –Be<sub>2</sub>H<sub>2</sub>– core structures by eliminating the high energy level HOMOs through insertion of an appropriate group. As the ultrashort Be–Be distances are expected to be maintained, it is better to “saturate” the –Be<sub>2</sub>H<sub>2</sub>– core using only one group. We therefore considered the methylene (–CH<sub>2</sub>–) and imino (–NH–) groups, which have been proved to be able to shorten the Be–Be distances in the Be<sub>2</sub>X<sub>2</sub> (X = C, N) rhombus through favourable electrostatic attractions.<sup>19</sup>

We thus added a –CH<sub>2</sub>– or –NH– group at the bridge position between the two beryllium atoms in **A1–C1**. According to our calculations, the addition of –CH<sub>2</sub>– to Be<sub>2</sub>X<sub>2</sub> (X = C, N) moieties led to the formation of minimum-energy structures **A1'–C1'** (see Fig. 3) at both the B3LYP/BS1 and B2PLYP-D3/BS1 levels. In contrast, when the –NH– group was added, saddle points, rather than minima, were obtained and the geometries adjusted by following the vectors of imaginary frequencies were distorted without ultrashort Be–Be distances. Thus, the structures with a bridging –NH– group were disregarded.

We noted that the HOMO energy of **A1'–C1'** of −3.23, −3.70, and −4.29 eV are 1.06, 1.29, and 1.09 eV lower than those of **A1–C1**, respectively. Since the LUMO energy levels of **A1'–C1'** are similar to or even higher than those of **A1–C1**, the HOMO–LUMO gaps in **A1'–C1'** are increased to 2.80, 2.73, and 3.58 eV and are 1.02, 1.41, and 1.32 eV larger than those of **A1–C1**, respectively. From electron excitation point of view, **A1'–C1'** should be more stable than **A1–C1**.

The orbital analyses results of **A1'** are given in Fig. 2. Those of **B1'** and **C1'** are similar to that of **A1'** and they are given in Fig. S1 and S2 in ESI.† As shown in these figures, **A1'–C1'** have two localized 2c-2e C–Be bonds instead of a 4c-2e  $\pi$ -bonds. The

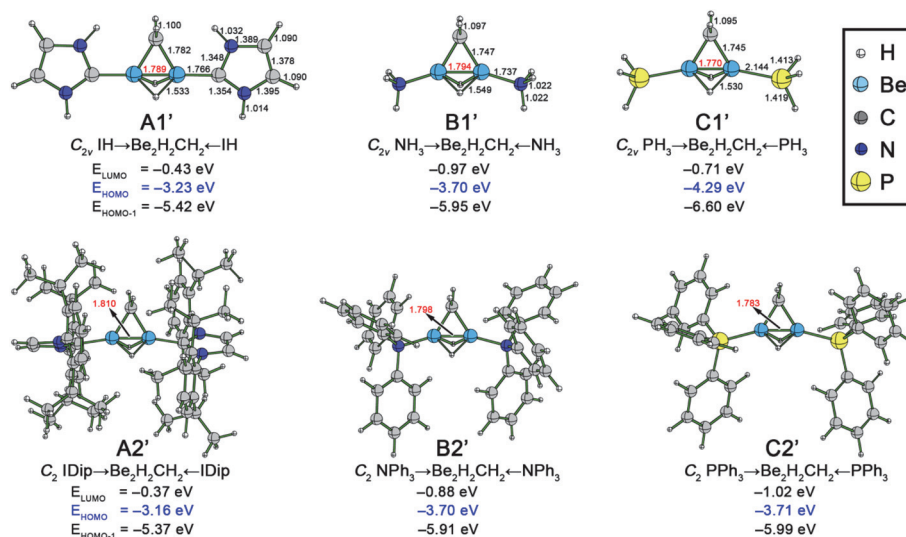


Fig. 3 CCSD(T)/BS1-optimized structures of **A1'–C1'** and B3LYP/BS1-optimized structures of **A2'–C2'**. The bond lengths or interatomic distances are given in angstrom.



HOMOs of **A1'**–**C1'** originate only from the combination of these two orbitals. After the addition of a  $-\text{CH}_2-$  group, each beryllium atom in the resultant **A1'**–**C1'** structures possesses a  $\text{C} \rightarrow \text{Be}$  2c-2e dative  $\sigma$ -bond, two Be–H–Be 3c-2e  $\sigma$ -bonds, and a classical C–Be 2c-2e  $\sigma$ -bond. Thus, all bonding orbitals around beryllium are  $\sigma$ -orbitals and hence, the core structures of **A1'**–**C1'** are “saturated”. Such a “saturation” process eliminated the unwanted high-energy  $\pi$ -shape HOMO and thus contributed to the stabilization of these species.

### Covalent bonding

The ultrashort Be–Be distances in **A1**–**C1** were achieved by forming three bonding orbitals. Interestingly, when one of these orbitals is broken, the Be–Be distance in **A1'**, **B1'**, and **C1'**, which are 1.789, 1.794, and 1.770 Å, respectively, still satisfy the criterion to be the ultrashort metal–metal distances. To find the reason why the beryllium–beryllium distances can be ultrashort, we performed the NBO analyses. The covalent bonding can be characterized by the Wiberg bond indices (WBI) provided by the NBO analyses. As shown in Table 1, before the addition of the  $-\text{CH}_2-$  group, the  $\text{WBI}_{\text{Be-X}}$  ( $X = \text{C}, \text{P}$ ) in **A1** and **C1** are 0.86 and 0.83, respectively, confirming the formation of Be–X single bonds; the  $\text{WBI}_{\text{Be-N}}$  in **B1** is only 0.44, suggesting that the covalent interactions between beryllium and nitrogen are relatively weak. The  $\text{WBI}_{\text{Be-H}}$  values in **A1**–**C1** are 0.47 or 0.48, validating the formation of Be–H–Be 3c-2e bonds. Since such 3c-2e bonds have a minor contribution to the WBI of the Be–Be bonds, the  $\text{WBI}_{\text{Be-Be}}$  values ranging from 0.78 to 1.26 are primarily due to their  $\pi$ -shape HOMOs.

In contrast, after the addition of the  $-\text{CH}_2-$  group, the  $\text{WBI}_{\text{Be-X}}$  values of **A1'**–**C1'** are somewhat smaller than those of **A1**–**C1**, suggesting that the  $X \rightarrow \text{Be}$  dative bonds are slightly weakened. The  $\text{WBI}_{\text{Be-H}}$  values in **A1'**–**C1'** are very close to those in **A1**–**C1**, consistent with the retained Be–H–Be 3c-2e bonds, while the  $\text{WBI}_{\text{Be-Be}}$  values are lowered to about 0.40 because the  $\pi$ -shape HOMOs are eliminated. Simultaneously, the WBI values for the bond between the carbon of the  $-\text{CH}_2-$  group and beryllium are 0.69, 0.75, and 0.75 in **A1'**, **B1'**, and

**C1'**, respectively, indicating the formation of localized Be–C single bonds. The covalent bonding analyses indicate that only two Be–H–Be 3c-2e bonds contribute to shortening of the Be–Be distances in **A1'**–**C1'**, which is not enough to achieve ultrashort Be–Be distances.

### Electrostatic interactions

We further studied the electrostatic interactions by analyzing the natural charge ( $Q$ ) distribution from the NBO results. As shown in Table 1, before the addition of the  $-\text{CH}_2-$  group, the natural charges on Be atoms and the atoms bonded to Be in **A1** and **C1** are small (from  $-0.17$  to  $+0.16|e|$ ), suggesting weak electrostatic interactions. Though the N atoms in **B1** bear a large negative charge of  $-1.09|e|$ , the Be atoms in **B1** are almost neutral ( $-0.02|e|$ ), indicating weak electrostatic interactions in **B1**. Such a result is consistent with the abovementioned conclusion that the ultrashort Be–Be distances in **A1**–**C1** are achieved by forming three bonding orbitals. However, after the addition of the  $-\text{CH}_2-$  group, though the charges on the H and X atoms hardly varied, those on the Be atoms became more positive (ranging from  $+0.14$  to  $+0.43|e|$ ). Simultaneously, the carbon atoms on the  $-\text{CH}_2-$  group bear large negative charges of  $-1.17$  to  $-1.32|e|$ , indicating that the electrostatic attractions between the beryllium atoms and the bridging carbon atom are significant. In addition to the retained Be–H–Be 3c-2e bonds, the favourable Coulomb attractions should be the key factor to achieve ultrashort Be–Be distances in **A1'**–**C1'**.

### Designing species with steric protection

The IH,  $\text{NH}_3$ , and  $\text{PH}_3$  ligands in **A1'**, **B1'**, and **C1'** can be replaced by their IDip,  $\text{NPh}_3$ , and  $\text{PPh}_3$  derivatives with bulky protection groups, respectively, leading to the formation of  $\text{IDip} \rightarrow \text{Be}_2\text{H}_2\text{CH}_2 \leftarrow \text{IDip}$  (**A2'**),  $\text{NPh}_3 \rightarrow \text{Be}_2\text{H}_2\text{CH}_2 \leftarrow \text{NPh}_3$  (**B2'**) and  $\text{PPh}_3 \rightarrow \text{Be}_2\text{H}_2\text{CH}_2 \leftarrow \text{PPh}_3$  (**C2'**) species. These species are computed to be minimum-energy structures with HOMO energies of 3.16, 3.70, and 3.71 eV at the B3LYP/BS1 level (see Fig. 3). The HOMO–LUMO gaps in **A2'**–**C2'** are 2.79, 2.82, and 2.69 eV, respectively, and are only slightly smaller

**Table 1** NBO results including the natural charges ( $Q$ , in  $|e|$ ) on Be, H, X ( $X = \text{C}, \text{N}, \text{P}$  for IH-,  $\text{NH}_3$ -, and  $\text{PH}_3$ -supported structures), and C of the  $-\text{CH}_2-$  moiety as well as the Wiberg bond indices (WBI) of the Be–Be, Be–H, Be–X, and Be–C bonds at the B3LYP/BS1 level

	$Q$				WBI			
	Be	H	X	C	Be–Be	Be–H	Be–X	Be–C
<b>A1</b>	0.06	–0.17	0.04	N/A	0.78	0.47	0.86	N/A
<b>B1</b>	–0.02	–0.19	–1.09	N/A	1.26	0.48	0.44	N/A
<b>C1</b>	–0.15	–0.14	0.16	N/A	1.03	0.48	0.83	N/A
<b>A1'</b>	0.25	–0.15	0.19	–1.32	0.40	0.46	0.65	0.69
<b>B1'</b>	0.43	–0.20	–1.07	–1.29	0.40	0.46	0.41	0.75
<b>C1'</b>	0.14	–0.13	0.21	–1.17	0.42	0.47	0.69	0.75
<b>A2</b>	0.15	–0.22	0.02	N/A	0.68	0.46	0.82	N/A
<b>B2</b>	0.20	–0.22	–0.63	N/A	0.91	0.45/0.46	0.31	N/A
<b>C2</b>	–0.12	–0.17	1.00	N/A	0.95	0.47	0.79	N/A
<b>A2'</b>	0.27	–0.18	0.18	–1.20	0.37	0.45/0.46	0.64	0.67
<b>B2'</b>	0.53	–0.21	–0.61	–1.38	0.36	0.45	0.27	0.69
<b>C2'</b>	0.16	–0.15	1.05	–1.24	0.38	0.46	0.68	0.74

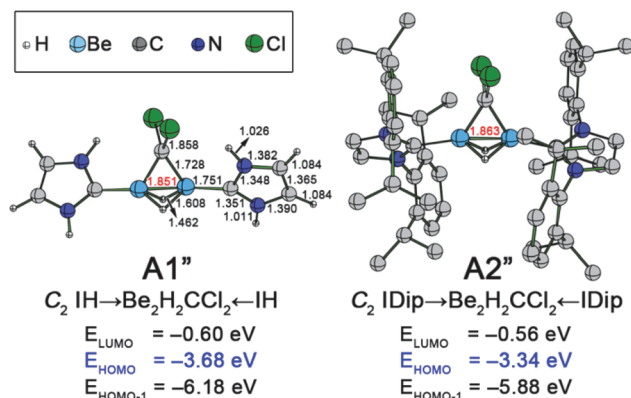


Fig. 4 B3LYP/BS1-optimized structures of **A1''** and **A2''**. The bond lengths or inter-atomic distances are given in angstrom.

than those in **A1'**–**C1'**. Moreover, the Be–Be distances in **A2'**–**C2'** are 1.810, 1.798, and 1.783 Å, respectively, which are only 0.021, 0.004, and 0.013 Å longer than the corresponding values in **A1'**–**C1'**. These results suggest that the addition of bulky groups not only retains the  $-\text{Be}_2\text{H}_2\text{CH}_2-$  core structures, but also introduces steric protection, which is beneficial to experimental realization.

### Results that may be useful for experimentalists

When synthesizing similar structures, our experimental colleagues may have a query: “where can the  $-\text{CH}_2-$  group come from?” In our opinion, the  $-\text{CH}_2-$  group in above species can be seen as a model for carbene, which can be introduced using the reaction employed to generate methylene from carbene. In experimental studies, methylene may also be replaced by various types of carbenes. Fig. 4 shows the optimized structures of  $\text{IH} \rightarrow \text{Be}_2\text{H}_2\text{CH}_2 \leftarrow \text{IH}$  (**A1''**) and  $\text{IDip} \rightarrow \text{Be}_2\text{H}_2\text{CH}_2 \leftarrow \text{IDip}$  (**A2''**) as the example. These structures are computed to be of minimum energy with Be–Be distances of 1.851 and 1.863 Å, respectively, at the B3LYP/BS1 level. The HOMO energy levels are found to be  $-3.68$  and  $-3.34$  eV, which are slightly lower than those of **A1'** and **A2'**, respectively. Simultaneously, the HOMO–LUMO gaps of 3.09 and 2.78 eV are also close to those of **A1'** and **A2'**, respectively, suggesting that **A1''** and **A2''** retain the good electronic structures found in the abovementioned species bearing a  $-\text{CH}_2-$  group.

## Conclusions

We found that the species with ultrashort Be–Be distances in the electron donating  $-\text{Be}_2\text{H}_2-$  moieties are not stable due to their delocalized high energy  $\pi$ -shape HOMOs. To eliminate the destabilization effect but maintain the ultrashort Be–Be distances, we proposed to combine the strategies of formation of multiple bonding orbitals and having favourable electrostatic attractions. Specifically, the addition of a  $-\text{CH}_2-$  group at the bridging position of the Be–Be axis not only directs the electrons from the delocalized high level  $\pi$ -shape orbitals into

localized  $\sigma$ -shape orbitals, but also retains the ultrashort Be–Be distances of 1.789, 1.794, and 1.770 Å in the newly designed  $\text{IH} \rightarrow \text{Be}_2\text{H}_2\text{CH}_2 \leftarrow \text{IH}$ ,  $\text{NH}_3 \rightarrow \text{Be}_2\text{H}_2\text{CH}_2 \leftarrow \text{NH}_3$ , and  $\text{PH}_3 \rightarrow \text{Be}_2\text{H}_2\text{CH}_2 \leftarrow \text{PH}_3$  species, respectively. Electronic structure analyses revealed that the beryllium atoms are saturated in these species, *i.e.*, the bonding orbitals around the beryllium atoms are all  $\sigma$ -orbitals. The ultrashort Be–Be distances were achieved by the combined shortening effects of two Be–H–Be 3c-2e  $\sigma$ -bonds and the favourable electrostatic attractions between the bridging carbon of the  $-\text{CH}_2-$  group and two beryllium atoms. When the electron donors have bulky protection groups, the corresponding  $\text{IDip} \rightarrow \text{Be}_2\text{H}_2\text{CH}_2 \leftarrow \text{IDip}$ ,  $\text{NPH}_3 \rightarrow \text{Be}_2\text{H}_2\text{CH}_2 \leftarrow \text{NPH}_3$ , and  $\text{PPh}_3 \rightarrow \text{Be}_2\text{H}_2\text{CH}_2 \leftarrow \text{PPh}_3$  structures are proposed as references for our experimental colleagues towards the realization of species with ultrashort metal–metal distances between main group metals.

## Conflicts of interest

There are no conflicts to declare.

## Acknowledgements

This project is supported by NSFC (Grant No. 21720102006, 21273140, 21471092, 21503252), the Special Program for Applied Research on Supercomputation of the NSFC-Guangdong Joint Fund (the second phase) (Grant No. U1501501), the Foundation of State Key Laboratory of Coal Conversion (Grant No. J17-18-610), the Program for the Outstanding Innovative Teams of Higher Learning Institutions of Shanxi Province, and the high performance computing platform of Shanxi University.

## Notes and references

- 1 F. A. Cotton, N. F. Curtis, C. B. Harris, B. F. G. Johnson, S. J. Lippard, J. T. Mague, W. R. Robinson and J. S. Wood, *Science*, 1964, **145**, 1306–1308.
- 2 T. Nguyen, A. D. Sutton, M. Brynda, J. C. Fettinger, G. J. Long and P. P. Power, *Science*, 2005, **310**, 844–847.
- 3 G. Frenking, *Science*, 2005, **310**, 796–797.
- 4 F. R. Wagner, A. Noor and R. Kempe, *Nat. Chem.*, 2009, **1**, 529–536.
- 5 A. Noor and R. Kempe, *Inorg. Chim. Acta*, 2015, **424**, 75–82.
- 6 K. A. Kreisel, G. P. A. Yap, O. Dmitrenko, C. R. Landis and K. H. Theopold, *J. Am. Chem. Soc.*, 2007, **129**, 14162–14163.
- 7 C.-W. Hsu, J.-S. K. Yu, C.-H. Yen, G.-H. Lee, Y. Wang and Y.-C. Tsai, *Angew. Chem., Int. Ed.*, 2008, **47**, 9933–9936.
- 8 A. Noor, F. R. Wagner and R. Kempe, *Angew. Chem., Int. Ed.*, 2008, **47**, 7246–7249.
- 9 Y.-C. Tsai, C.-W. Hsu, J.-S. K. Yu, G.-H. Lee, Y. Wang and T.-S. Kuo, *Angew. Chem., Int. Ed.*, 2008, **47**, 7250–7253.
- 10 A. Noor, G. Glatz, R. Mueller, M. Kaupp, S. Demeshko and R. Kempe, *Z. Anorg. Allg. Chem.*, 2009, **635**, 1149–1152.

- 11 A. Noor and R. Kempe, *Chem. Rec.*, 2010, **10**, 413–416.
- 12 A. Noor, T. Bauer, T. K. Todorova, B. Weber, L. Gagliardi and R. Kempe, *Chem. – Eur. J.*, 2013, **19**, 9825–9832.
- 13 G. Merino, K. J. Donald, J. S. D'Acchioli and R. Hoffmann, *J. Am. Chem. Soc.*, 2007, **129**, 15295–15302.
- 14 G. Frenking and R. Tonner, *Nature*, 2007, **446**, 276–277.
- 15 F. Weinhold and C. R. Landis, *Science*, 2007, **316**, 61–63.
- 16 B. O. Roos, A. C. Borin and L. Gagliardi, *Angew. Chem., Int. Ed.*, 2007, **46**, 1469–1472.
- 17 M. Brynda, L. Gagliardi and O. R. Bjorn, *Chem. Phys. Lett.*, 2009, **471**, 1–10.
- 18 Z.-H. Cui, W.-S. Yang, L. Zhao, Y.-H. Ding and G. Frenking, *Angew. Chem., Int. Ed.*, 2016, **55**, 7841–7846.
- 19 C. Yuan, X.-F. Zhao, Y.-B. Wu and X. Wang, *Angew. Chem., Int. Ed.*, 2016, **55**, 15651–15655.
- 20 Q. Zhang, W.-L. Li, L. Zhao, M. Chen, M. Zhou, J. Li and G. Frenking, *Chem. – Eur. J.*, 2017, **23**, 2035–2039.
- 21 S. Grimme, S. Ehrlich and L. Goerigk, *J. Comput. Chem.*, 2011, **32**, 1456–1465.
- 22 L. Goerigk and S. Grimme, *J. Chem. Theory Comput.*, 2011, **7**, 291–309.
- 23 A. E. Reed, L. A. Curtiss and F. Weinhold, *Chem. Rev.*, 1988, **88**, 899–926.
- 24 D. Y. Zubarev and A. I. Boldyrev, *J. Org. Chem.*, 2008, **73**, 9251–9258.
- 25 D. Y. Zubarev and A. I. Boldyrev, *Phys. Chem. Chem. Phys.*, 2008, **10**, 5207–5217.
- 26 The AdNDP program can be downloaded at <http://ion.chem.usu.edu/~boldyrev/adndp.php>.
- 27 H.-J. Werner, et al., in *MolPro 2012.1*, University College Cardiff Consultants Limited, Cardiff UK, 2012.
- 28 M. J. Frisch, et al., in *Gaussian 09 Revision D.01*, Gaussian Inc., Wallingford CT, 2013.
- 29 S. Grimme and P. R. Schreiner, *Angew. Chem., Int. Ed.*, 2011, **50**, 12639–12642.